Influence of Permeant Ions on Voltage Sensor Function in the Kv2.1 Potassium Channel

Joseph F. Consiglio and Stephen J. Korn

Department of Physiology and Neurobiology, University of Connecticut, Storrs, CT 06269

ABSTRACT We previously demonstrated that the outer vestibule of activated Kv2.1 potassium channels can be in one of two conformations, and that K^+ occupancy of a specific selectivity filter site determines which conformation the outer vestibule is in. These different outer vestibule conformations result in different sensitivities to internal and external TEA, different inactivation rates, and different macroscopic conductances. The $[K^+]$-dependent switch in outer vestibule conformation is also associated with a change in rate of channel activation. In this paper, we examined the mechanism by which changes in $[K^+]$ modulate the rate of channel activation. Elevation of symmetrical $[K^+]$ or $[Rb^+]$ from 0 to 3 mM doubled the rate of on-gating charge movement (Q_{on}), measured at 0 mV. Cs^+ produced an identical effect, but required 40-fold higher concentrations. All three permeant ions occupied the selectivity filter over the 0.03–3 mM range, so simple occupancy of the selectivity filter was not sufficient to produce the change in Q_{on}. However, for each of these permeant ions, the speeding of Q_{on} occurred with the same concentration dependence as the switch between outer vestibule conformations. Neutralization of an amino acid (K356) in the outer vestibule, which abolishes the modulation of channel pharmacology and ionic currents by the K^+-dependent reorientation of the outer vestibule, also abolished the K^+-dependence of Q_{on}. Together, the data indicate that the K^+-dependent reorientation in the outer vestibule was responsible for the change in Q_{on}. Moreover, similar $[K^+]$-dependence and effects of mutagenesis indicate that the K^+-dependent change in rate of Q_{on} can account for the modulation of ionic current activation rate. Simple kinetic analysis suggested that K^+ reduced an energy barrier for voltage sensor movement. These results provide strong evidence for a direct functional interaction, which is modulated by permeant ions acting at the selectivity filter, between the outer vestibule of the Kv2.1 potassium channel and the voltage sensor.

KEY WORDS: activation • gating currents • conformational change • outer vestibule • selectivity filter

INTRODUCTION

Opening of voltage-gated K^+ channels depends on the interaction between the voltage sensor and a voltage-sensitive gate within the pore. Upon depolarization, positive gating charge within the channel protein moves in the outward direction (Hodgkin and Huxley, 1952; Armstrong and Bezanilla, 1974). The region of the channel that contains most of these gating charges, and therefore primarily constitutes the voltage sensor, is the S4 transmembrane domain (Aggarwal and MacKinnon, 1996; Seoh et al., 1996). As the S4 domain translocates in the outward direction, the activation gate within the conduction pathway opens, and allows ions to flow through the pore. Abundant evidence has demonstrated that the primary, voltage-sensitive activation gate lies at the cytoplasmic end of the conduction pathway (Armstrong and Hille, 1972; Holmgren et al., 1997, 1998; Liu et al., 1997; del Camino and Yellen, 2001; Hackos et al., 2002). Although the details remain to be fully worked out, the S4 domain appears to be linked to the activation gate at the cytoplasmic end of the channel protein (Lu et al., 2002; Tristani-Firouzi et al., 2002; Ding and Horn, 2003).

Cysteine modification and cross-linking experiments indicate that the S4 domain is also within very close proximity of the outer vestibule (Elinder et al., 2001a,b; Broomand et al., 2003; Gandhi et al., 2003; Laine et al., 2003; Neale et al., 2003). The possibility that this close proximity is functionally important is suggested by fluorescence measurements that demonstrated a link between movement of the S4 domain and slow inactivation, which involves a conformational change in the outer vestibule (Yellen et al., 1994; Liu et al., 1996; Loots and Isacoff, 2000). However, whether the association between S4 movement and slow inactivation results from a direct interaction between the S4 domain and outer vestibule or via a more indirect mechanism is not known (see Elinder et al., 2001b; Broomand et al., 2003).

Several types of evidence have raised the possibility that the outer vestibule and/or selectivity filter might

Address correspondence to Stephen Korn, Department of Physiology and Neurobiology, Box U-156, University of Connecticut, 3107 Horsebarn Hill Rd., Storrs, CT 06269. Fax: (860) 486-3303; email: stephen.korn@uconn.edu

Abbreviation used in this paper: MTSET, [2-(trimethylammonium)ethyl] methanethiosulfonate.

J. Gen. Physiol. © The Rockefeller University Press • 0022-1295/2004/04/387/14 $8.00
Volume 123 April 2004 387–400
http://www.jgp.org/cgi/doi/10.1085/jgp.200308976

also be involved in the activation process. First, it is now clear that the selectivity filter is a dynamic region of the channel (Ikeda and Korn, 1995; Liu et al., 1996; Kiss et al., 1999; Wang et al., 2000; Zhou et al., 2001). Second, fluorescence measurements have demonstrated that conformational changes occur in the outer vestibule during activation (Cha and Bezanilla, 1997). Third, site-directed mutagenesis near the selectivity filter region of the channel alters the kinetics of activation gating (Liu and Joho, 1998; Zheng and Sigworth, 1998). Fourth, open-close gating transitions continue to occur when the cytoplasmic activation gate is uncoupled from the S4 domain (Bao et al., 1999). Finally, several studies suggest that the primary activation gate in inward rectifier K^+ channels and cyclic nucleotide–gated channels, which are closely related to Kv channels, may be associated with the selectivity filter region (Sun et al., 1996; Flynn and Zagotta, 2001; Lu et al., 2001a,b; So et al., 2001; Proks et al., 2003). Together, these data provide compelling circumstantial evidence that a second gate, near the selectivity filter and/or outer vestibule region, might contribute to the activation process in Kv channels. The ability of the S4 domain to move to within several angstroms of the outer vestibule suggests the possibility that it may influence gating transitions associated with the selectivity filter and/or outer vestibule.

We recently demonstrated that the outer vestibule of activated Kv2.1 potassium channels can be in one of two conformations, and that the occupancy by K^+ of a specific selectivity filter site determines which conformation the outer vestibule is in (Immke et al., 1999; Immke and Korn, 2000). These different conformations are associated with differences in channel pharmacology, current magnitude and inactivation rate (Immke et al., 1999; Immke and Korn, 2000; Wood and Korn, 2000). In this manuscript, we demonstrate that occupancy of this same selectivity filter site by permeating ions influences the rate of on-gating charge movement, and consequently, the rate of ionic current activation. Moreover, we show that this effect of ions within the conduction pathway influences the rate of gating charge movement as a result of the previously described K^+-dependent change in outer vestibule conformation. These results indicate that changes in outer vestibule conformation, controlled by ion occupancy of a site within the pore, can influence the movement of the voltage sensor during the activation process.

MATERIALS AND METHODS

Molecular Biology and Channel Expression

Experiments were done on the wild-type and several mutant Kv2.1 channels. Mutations were made with the Quickchange site-directed mutagenesis kit (Stratagene), as described previously (Immke et al., 1999). Mutations were confirmed by sequence analysis. K^+ channel cDNA was subcloned into the pcDNA3.1 expression vector and channels expressed in the human embryonic kidney cell line, HEK 293 (American Type Culture Collection). Cells were maintained in DMEM plus 10% fetal bovine serum (Hyclone Laboratories, Inc.) with 1% penicillin/streptomycin. Cells (2×10^6 cells/ml) were cotransfected by electroporation (Bio-Rad Gene Pulser II @ 220 V, 350 μF) with K^+ channel expression plasmid (0.5–10 μg/0.2 ml) and CD8 expression plasmid (1 μg/0.2 ml). After electroporation, cells were plated on glass coverslips submerged in maintenance media. Electrophysiological recordings were made 18–28 h later. On the day of recording, cells were washed with fresh media and incubated with Dynabeads M450 conjugated with antibody to CD8 (0.5 μl/ml; Dynal). Cells that expressed CD8 became coated with beads, which allowed visualization of transfected cells (Jurman et al., 1994).

Electrophysiology

Currents were recorded at room temperature in the whole cell patch clamp configuration. Patch pipets were fabricated from N51A glass (Garner Glass Co.), coated with Sylgard, and firepolished. Currents were collected with an Axopatch 1D amplifier, pClamp 9 software, and a Digidata 1322A A/D board (Axon Instruments, Inc.). Currents were filtered at 2 KHz and sampled at 40–200 μs/pt. Series resistance ranged from 0.5 to 2.5 MΩ and was compensated 80–90%. The holding potential was −80 mV, and depolarizing stimuli were presented once every 6–10 s, depending on the experiment. Gating currents were collected using a P/4 protocol (voltage was stepped from −80 to −100 mV at 5.5 Hz). All displayed gating currents are averages of 5–12 currents evoked consecutively. In most experiments, gating currents were recorded at 0 mV with symmetrical internal and external permeant ion concentrations. This protocol was used for three reasons. First, 0 mV was approximately centered on the rising phase of the Q-V curve. Second, recording gating currents at the reversal potential (0 mV) eliminated contamination from ionic currents when permeant ions were used. Third, recording at a reversal potential of 0 mV avoided complications of voltage-dependent influences on permeant ion access to sites within the pore from both internal and external solutions.

Data were analyzed with Clampfit 9 (Axon Instruments, Inc.); curve fitting and significance testing (unpaired Student's *t* test) were done with SigmaPlot 8.0 (SPSS, Inc.). Gating currents were integrated with both SigmaPlot and Origin 6.0 (Microcal Software, Inc.), which gave identical results. All plotted data are represented as mean ± SEM, with the number of data points denoted by *n*. EC_{50} values for concentration-response curves were determined from the best fit of the mean data. Consequently, *n* values are expressed as a range, which reflects a different number of cells examined for different data points on the curve. Differences between means were considered statistically significant if p values in unpaired Student's *t* tests were <0.05.

Curve Fitting

Gating currents were fit to a single exponential function. In all cases, cursors were set at the peak of the gating current and at the end of the depolarization that activated the gating current. As will become clear later in the manuscript, the mechanistic explanation for our data suggests that currents should decay with two exponentials (having time constants of ∼2.5 and ∼5 ms), with weightings that depend on the percentage of channels in each of two proposed conformational states of the channel. However, a two exponential function with these time constants cannot be distinguished from a single exponential function of intermediate time constant. Consequently, we chose to use single exponential functions to quantify gating current decay. These

produced good fits (see Fig. 2 A) and were suitable for the purposes of our analysis and interpretations.

Concentration-response curves were fit with the equation:

$$y = \min + [(\max - \min)/1 + 10(\log EC_{50} - x)n], \quad (1)$$

where max is the maximum value on the ordinate, min is the minimum value on the ordinate, x is the drug concentration, and n is a power value that corresponds to a Hill-type coefficient. During curve fitting, max, min, EC_{50}, and n were free parameters. Q-V curves were fit to the Boltzmann equation, $y = 1/(1 + \exp((V_{1/2} - V)/r))$, where Vh is the voltage of half maximal activation, V is the membrane voltage, and r is a slope value.

Electrophysiological Solutions

Currents were recorded in a constantly flowing, gravity-fed bath. Solutions were placed in one of six reservoirs, each of which fed via PE tubing into a Delrin perfusion manifold. Solution exited the manifold via PE tubing (~580-μm diameter). Flow rates were carefully matched among barrels. Cells were lifted off of the dish before recording and placed ~20 μm from the tip of the perfusion tube. One solution was always flowing, and solutions were switched manually (solution exchange was complete within 5–10 s). Control internal solutions contained (in mM): 130 XCl (X = a combination of K^+, Na^+ and/or NMG^+), 10 HEPES, 10 EGTA, 1 $CaCl_2$, 4 $MgCl_2$; pH 7.3, osmolality 285. Control external solutions contained (in mM): 160 XCl, 10 HEPES, 10 glucose, 2 $CaCl_2$, and 1 $MgCl_2$; pH 7.3, osmolality 325. The $[K^+]$ and $[Na^+]$ used in each experiment are described in the text (NMG^+ provided the balance of the [monovalent cation] present).

MTSET Experiments

In some experiments (Figs. 8–10), channels containing a cysteine at position 356 or 379 were modified by [2-(trimethylammonium)ethyl] methanethiosulfonate (MTSET; Toronto Research Chemicals). MTSET solutions were made by adding dry powder to the external recording solution to a final MTSET concentration of 2 mM (Fig. 8) or by serial dilution to 100 μM from a 5-mM stock solution in ice cold water (Figs. 9 and 10). MTSET was applied in one of two ways. Either MTSET was perfused onto the cell at the time of recording or cells were preincubated with MTSET immediately before recording. Both approaches produced identical results.

RESULTS

We previously demonstrated that currents through the Kv2.1 potassium channel are potentiated upon elevation of external $[K^+]$ (Wood and Korn, 2000). This effect is illustrated in Fig. 1 A. In addition to causing an increase in current magnitude, elevation of $[K^+]$ increased the rate of ionic current activation. This is most clearly observed by the normalized set of currents in Fig. 1 B. With 100 mM internal K^+, elevation of external $[K^+]$ from 0 to 10 mM nearly doubled the rate of activation for currents activated by depolarization to 0 mV (Fig. 1 C).

The K^+-dependent potentiation of current magnitude is associated with a change in outer vestibule conformation (Wood and Korn, 2000). Similarly, the different activation rates could also be associated with the two different K^+-dependent outer vestibule conformations. Alternatively, the different activation rates may be

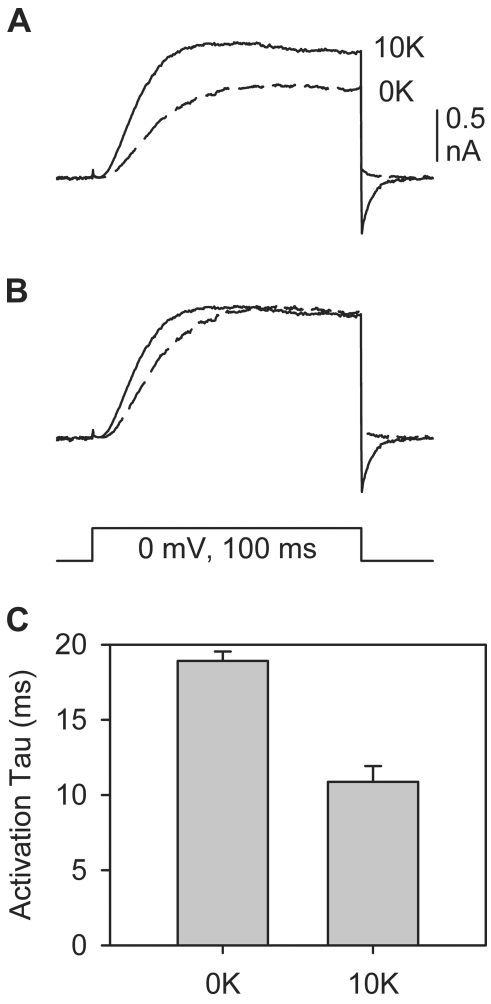

FIGURE 1. K^+-dependent increase in current magnitude and activation rate. (A) Two superimposed traces recorded consecutively from a single cell illustrate currents activated in the presence of 0 mM external K^+ (dashed line) and 10 mM external K^+ (solid line). (B) Traces in A were normalized to the peak current magnitude to illustrate the speeding of activation in higher $[K^+]$. (C) Plot of activation time constants, measured from single exponential fits of the rising phase of the current. Each bar represents the mean ± SEM from eight cells (0 and 10 K^+ values were obtained in pairs from the same cells).

completely independent of the change in outer vestibule conformation, but affected by an action of K^+ somewhere else within the pore. For each of these possibilities, the change in activation rate could occur via either of two mechanisms. First, the increased activation rate could be associated with an increased rate of voltage sensor movement. Alternatively, the increased activation rate might be due to a change in pore gating, independent of voltage sensor movement.

In the experiments below, we examined the involvement of the voltage sensor in this speeding of activation, and tested whether the K^+ sensitivity of activation rate resulted from the modulation of outer vestibule conformation by K^+ occupancy of the selectivity filter.

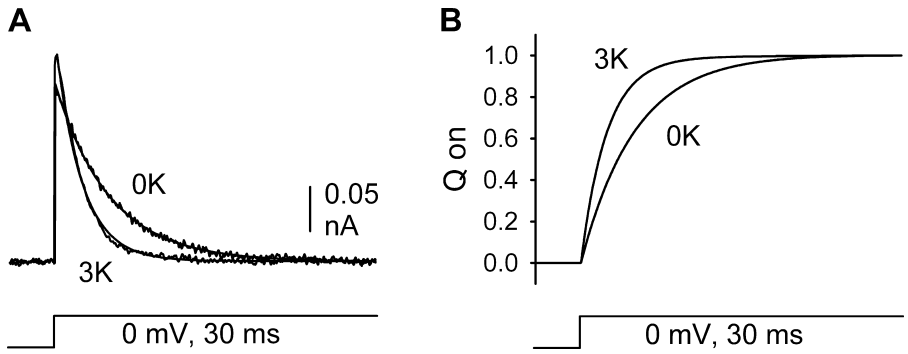

FIGURE 2. Speeding of gating charge movement by K^+. (A) Gating currents recorded from two different cells, one recorded in the absence of K^+ (or any other permeant ion; 0 K) and one recorded with 3 mM internal and external K^+ (3 K). Superimposed on each current trace is the single exponential fit used to obtain the time constant of decay. (B) The area under the currents in A was measured to obtain a plot of the cumulative rate of charge movement. These were then normalized to the maximum charge movement to give a plot of the fractional Q_{on}. Time constants, calculated from single exponential fits, were nearly identical for the decay phase of the currents in A and the Q_{on} curves in B (4.86 and 4.85 ms [0 K], 2.36 and 2.37 ms [3 K]).

Influence of Permeant Ions on Gating Currents

Fig. 2 A illustrates two superimposed gating currents, recorded at 0 mV, from two different cells (single exponential fits are superimposed on each gating current). One gating current was recorded in the complete absence of internal or external permeant ions (0 K). The other trace was recorded with 3 mM internal and external K^+ (3 K). Clearly, the rate of decay of the gating current was faster when recorded in 3 mM K^+. Gating currents were reasonably well fit by single exponential functions, with decay time constants of 4.83 ± 0.19 ms (n = 11; 0 K) and 2.77 ± 0.18 ms (n = 6; 3 K).

Fig. 2 B illustrates the cumulative charge movement, derived from the same data as in Fig. 2 A. This transformation also utilizes the rising phase of the gating current, and therefore includes information neglected when fitting only the decay of the raw gating currents. The time constants obtained from exponential fits to these two curves (4.85 ms [0 K], 2.37 ms [3 K]) were essentially identical to those obtained from the decay phase of the two currents illustrated in Fig. 2 A (4.86 ms [0 K], 2.36 ms [3 K]). Consequently, for the remainder of the paper, we calculated time constants from fits of gating current decay.

Fig. 3 A illustrates gating currents recorded in the absence of permeant ions and in the presence of symmetrical concentrations of internal and external K^+, Rb^+, or Cs^+. The rate of gating charge movement (Q_{on}) was increased similarly by 3 mM K^+ and 3 mM Rb^+. In contrast, 3 mM Cs^+ was without effect. However, elevation of [Cs^+] to 100 mM increased the rate of Q_{on} to that produced by 3 mM K^+ and 3 mM Rb^+. Fig. 3 B illustrates complete concentration-response curves for the influence of the three permeant ions on Q_{on}. The concentration-dependent influences of K^+ and Rb^+ were nearly identical, with calculated EC_{50}s of 0.86 ± 0.01 (n = 5–11) and 1.13 ± 0.06 (n = 3–6) (Fig. 3 B). While just as efficacious, Cs^+ was much less potent, with a calculated EC_{50} of 41.5 ± 0.05 (n = 3–6).

As described previously (Immke and Korn, 2000; Wood and Korn, 2000), the influence of K^+ on ionic current magnitude involved the occupancy of a specific selectivity filter site. The difference in permeant ion potency observed in Fig. 3 presented an opportunity to

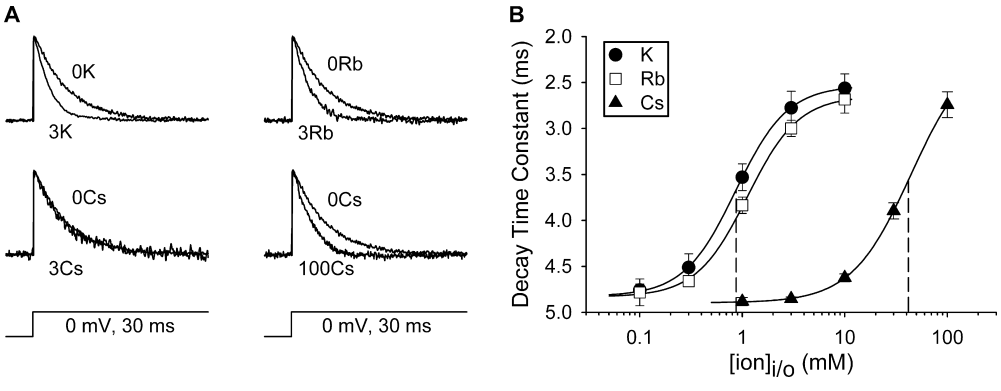

FIGURE 3. Concentration-dependent speeding of gating charge movement by different permeant ions. (A) Pairs of traces illustrate gating currents recorded at 0 mV in the absence of permeant ions and the presence of symmetrical 3 mM K^+, 3 mM Rb^+, 3 mM Cs^+, and 100 mM Cs^+. Raw gating current magnitudes ranged from 40 pA (3 Cs) to 270 pA (100 Cs). (B) Concentration-response curves for speeding of Q_{on} by the 3 different permeant ions. Data were fit by Eq. 1 (MATERIALS AND METHODS). Calculated EC_{50} values for K^+, Rb^+, and Cs^+ were: 0.86 ± 0.01 mM (n = 5–11), 1.13 ± 0.06 mM (n = 3–6) and 41.5 ± 0.05 (n = 3–6). The calculated minimum time constant (saturation of the concentration-response curve) for Cs^+ data was 2.12 ms. Calculated slope values were 1.72, 1.74, and 1.51. Vertical dashed lines are drawn at the calculated EC_{50} values for K^+ and Cs^+.

evaluate the involvement of specific selectivity filter sites on gating charge movement.

Involvement of the Selectivity Filter Site that Controlled Outer Vestibule Conformation

First, we asked whether Cs^+ could occupy the selectivity filter at concentrations similar to those required for occupancy by K^+ and Rb^+. To test this, we examined the ability of the three permeant ions to block Na^+ currents through the channel. Fig. 4 A illustrates inward Na^+ currents in the absence (Na) and presence of 1 mM K^+ (panel 1), Rb^+ (panel 2), or Cs^+ (panel 3). Fig. 4 B illustrates the concentration-dependent block of Na^+ current by each of the three ions. All three ions blocked Na^+ currents with identical concentration dependence, which indicates that all three ions were able to singly occupy the selectivity filter at identical low concentrations.

We then asked whether Cs^+ occupied the specific selectivity filter site that controlled outer vestibule conformation at the same concentrations as K^+ and Rb^+. Occupancy of this specific site not only influences ionic current magnitude, but also affects TEA efficacy (Immke et al., 1999; Immke and Korn, 2000). In K^+-conducting channels, TEA can block the channel only if this specific selectivity filter site is occupied by K^+. TEA cannot block the channel if this site is unoccupied or if Na^+ is the only permeant ion used. Fig. 4 C illustrates three pairs of currents. The control traces illustrate inward currents recorded in the presence of 130 mM Na^+ plus 1 mM K^+ (panel 1), Na^+ plus 1 mM Rb^+ (panel 2) or Na^+ plus 1 mM Cs^+ (panel 3). The second trace illustrates block of the current by 30 mM TEA. TEA blocked currents in the presence of K^+ and Rb^+ almost identically. However, TEA did not block currents in the presence of 1 mM Cs^+. Concentration-response curves for permeant ion concentrations up to 10 mM are illustrated in Fig. 4 D. K^+ and Rb^+ allowed TEA to block with identical concentration dependence, which indicates that occupancy of the specific selectivity filter site that controls outer vestibule conformation was identical for K^+ and Rb^+. In contrast, at [Cs^+] up to 10 mM, there was little TEA block, which suggested that even though Cs^+ could occupy the selectivity filter at these concentrations, it did not occupy the specific site that controlled outer vestibule conformation. This conclusion was confirmed by the somewhat different experiment in Fig. 5.

For Fig. 5, TEA block was examined in the presence of symmetrical ion concentrations (no Na^+ was present), so that results could be compared with the gating current data in Fig. 3. For K^+ and Rb^+, we examined block by 3 mM TEA for a complete range of permeant ion concentrations. Maximum block by TEA was identical for the two ions (see Fig. 5 legend). Moreover, the

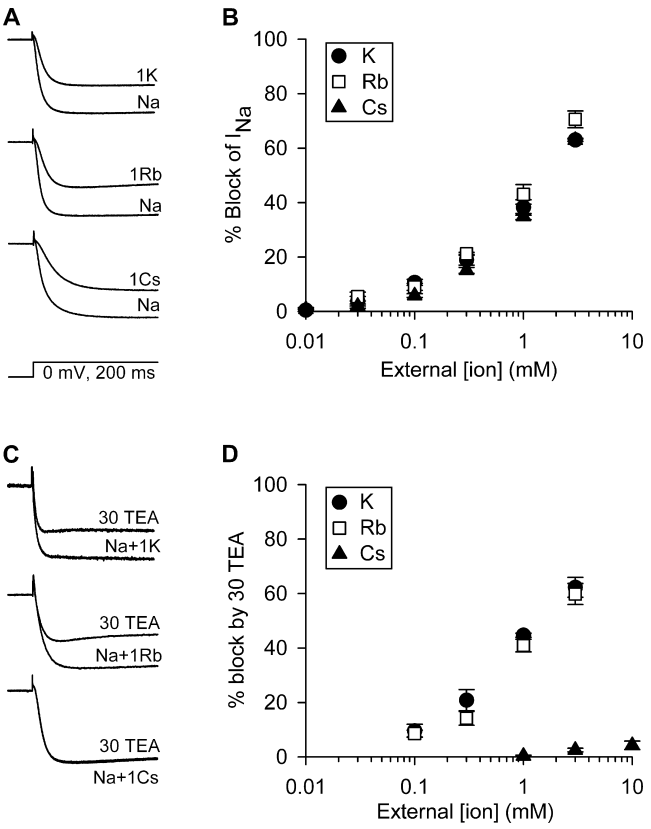

FIGURE 4. Interaction of permeant ions with the selectivity filter. (A) Pairs of consecutively recorded traces illustrate inward currents carried by 130 mM external Na^+ (Na) or 130 mM Na^+ plus 1 mM K^+, Rb^+, or Cs^+. Inward Na^+ current magnitude was 2,400, 2,500, and 1,800 pA in the three pairs of records shown. (B) Concentration-dependent block of inward current by K^+, Rb^+, or Cs^+, applied externally. Data points represent the mean ± SEM of 3–5 cells. (C) Pairs of consecutively recorded traces. The control inward current was recorded in the presence of 130 mM Na^+ plus 1 mM K^+, Rb^+, or Cs^+. The second trace illustrates currents evoked following equimolar replacement of 30 mM external NMG+ with TEA. Inward current magnitude in the absence of TEA was 420, 900, and 3,200 pA in the three pairs of records shown. (D) Block of inward current by 30 mM TEA in the presence of the indicated concentration of external K^+, Rb^+, or Cs^+. Data points represent the mean ± SEM of 3–6 cells.

EC_{50}s at which K^+ and Rb^+ allowed TEA to block were essentially identical for the two ions (Fig. 5). These results indicate that, with symmetrical ion concentrations, K^+ and Rb^+ occupied the selectivity filter site that controlled outer vestibule conformation identically.

In contrast, a much higher [Cs^+] was required for TEA to block the channel (Fig. 5; to increase resolution in the presence of Cs^+, 100 mM TEA was used—see legend). The EC_{50} for Cs^+ was 44.8 ± 0.9 mM (n = 3–6), which is virtually identical to the EC_{50} at which Cs^+ increased the rate of Q_{on} (see Fig. 3). Indeed, comparison of the data in Fig. 3 B and 5 illustrates that the EC_{50}s for the speeding of Q_{on} and the promotion of

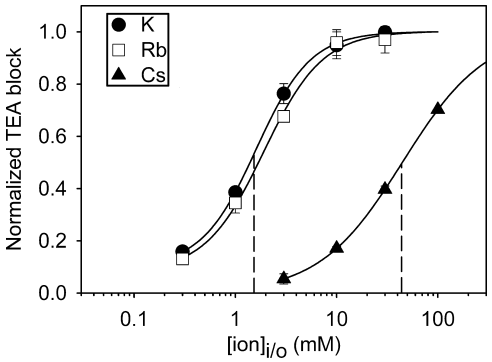

FIGURE 5. Permeant ion dependence of TEA sensitivity. Ion concentrations on the abscissa represent the concentration of both internal and external permeant ion. Currents were evoked by depolarization to +40 mV, and then TEA was applied to block the current. Changes in block represent changes in TEA efficacy, not potency (see Immke and Korn, 2000). 3 mM TEA was used to block K^+ and Rb^+ currents; 100 mM TEA was used to block Cs^+ currents. Data points represent the mean ± SEM of 3–6 cells, from which a single best fit was calculated using Eq. 1. The calculated maximum block by 3 mM TEA was 32.8 ± 0.3% for K^+ currents and 33.3 ± 1.4% for Rb^+ currents. The calculated maximum block by 100 mM TEA in the presence of Cs^+ was 90.7 ± 1.0%. Calculated EC_{50} values for K^+, Rb^+, and Cs^+ were: 1.6 ± 0.1 mM, 1.9 ± 0.3 mM, and 44.8 ± 0.9 mM. Vertical dashed lines are drawn at the calculated EC_{50} values for K^+ and Cs^+ concentration-response curves.

TEA block were virtually identical for each of the three permeant cations. These results strongly support the conclusion that occupancy of the specific selectivity filter site that controls outer vestibule conformation also modulated the rate of gating charge movement.

Involvement of the Outer Vestibule Conformational Change in Speeding of Q_{on}

The K^+-dependent increases in TEA efficacy, ionic current magnitude, and ionic current activation rate are abolished specifically by mutation of the outer vestibule lysine at position 356 to a glycine (Immke and Korn, 2000; Wood and Korn, 2000). In contrast, mutation of the other exposed outer vestibule lysine, at position 382, to a valine had no effect on the K^+ dependence of these functional parameters. Mutation of K356 does not abolish the K^+-dependent conformational change itself (Immke et al., 1999). Rather, the effects of different outer vestibule conformations on TEA efficacy and ionic current properties appear to depend specifically on the reorientation of the K356 sidechain within the outer vestibule. Thus, we tested whether the $[K^+]$-dependent increase in rate of gating charge movement was similarly associated with reorientation of K356 by determining the $[K^+]$ dependence in mutant channels that lacked one or more outer vestibule lysines.

First, we examined whether outer vestibule mutations influenced gating charge movement in the absence of permeant ions. Fig. 6 illustrates gating currents recorded at +50 mV (Fig. 6 A) and −10 mV (Fig. 6 B) from two channels, wild-type Kv2.1 and the well-characterized mutant channel, Kv2.1 K356G K382V. Fig. 6 C illustrates the complete Q-V curve for each of these two channels. These results demonstrate that, in the absence of K^+, the kinetics of the gating current and the voltage dependence of gating charge movement were unaffected by these two mutations.

We next examined whether mutation of one or more outer vestibule lysines eliminated the $[K^+]$-dependent change in rate of gating charge movement. Fig. 7, A and B, illustrate that 3 mM K^+ had essentially no effect on the rate of gating charge movement in Kv2.1 K356G K382V. Fig. 7, C and D, illustrate the effect of single lysine mutations. The K^+-dependent effect remained in Kv2.1 K382V (which contained the lysine at position 356; Fig. 7 C) and was completely abolished by the K356G mutation alone (Fig. 7 D). As shown below (Fig. 9), changing the charge on the residue at position 379 in the outer vestibule also had no impact on gating current characteristics in either the presence or absence of K^+. Thus, it was not merely the presence of exposed positive charges in the outer vestibule that influenced gating currents. Rather, these data strongly suggest that the $[K^+]$-dependent change in rate of gating charge movement depended specifically on the K^+-dependent reorientation of the lysine at position 356.

Finally, we examined the necessity of the lysine-like properties of the amino acid side chain at position 356. Just as with the K356G mutation, mutation of K356 to a cysteine abolished the K^+-dependent speeding of Q_{on} (Fig. 8 A, top, and B). However, modification of the position 356 cysteine with MTSET, which produces a sidechain quite similar to that of a lysine, restored the K^+-dependent speeding of Q_{on} (Figs. 8 A, bottom, B). Modification of C356 with MTSET produced no change in Q_{on} in 0 mM K^+ (Fig. 8 B). These results demonstrate that the outer vestibule mutations did not fundamentally alter the conformation or K^+-dependent reorientation of the outer vestibule. Rather, mutation-based abolition of the K^+-dependence of gating current rate resulted simply from the change in amino acid sidechain at position 356.

Together, the results in Figs. 2–8 demonstrate that changes in $[K^+]$ influence the rate of gating charge movement via the same mechanism that is involved in modulation of TEA efficacy and potentiation of ionic current magnitude. Thus, the increase in rate of gating charge movement is associated with the occupancy of the specific selectivity filter site that appears to regulate a switch in outer vestibule conformation. Moreover, the influence of K^+ on gating currents depends on the pres-

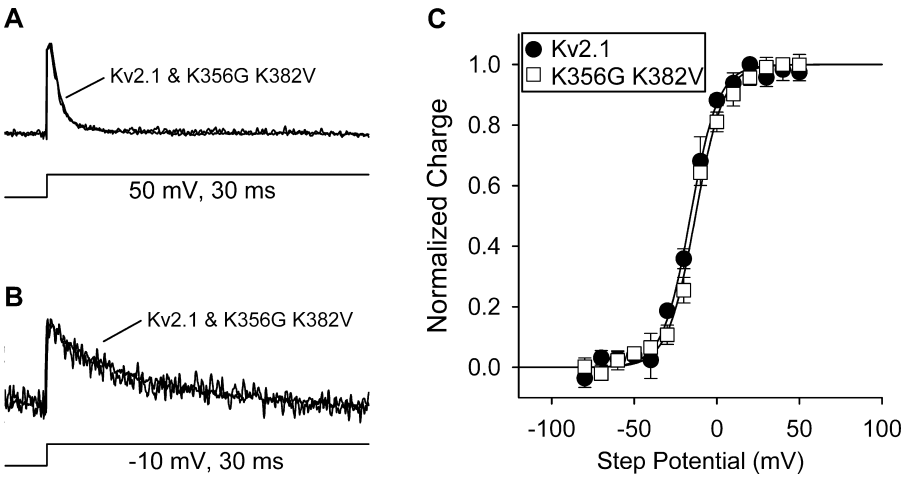

FIGURE 6. Comparison of Q-V curves for wild-type Kv2.1 and the mutant, Kv2.1 K356G K382V. (A and B) Superimposed (normalized) gating currents from two different cells, one that contained Kv2.1 channels and one that contained Kv2.1 K356G K382V. Panel A illustrates currents evoked by depolarization to +50 mV, and panel B illustrates currents evoked by depolarization to −10 mV. (C) Complete Q-V curves for the two channels, recorded in the absence of permeant ions. Normalized charge, plotted on the ordinate, was calculated from the integrated gating currents and fit by the Boltzmann equation described in MATERIALS AND METHODS. Data points represent the mean ± SEM of 3–4 cells at each potential. The calculated $V_{1/2}$ values for Kv2.1 and the mutant channel were 15.1 ± 1.5 mV and 12.8 ± 0.8 mV. Slope values were 8.4 and 8.5, respectively.

ence of the lysine at position 356, and is associated with the change in outer vestibule conformation that apparently reorients K356.

K^+ Does Not Shift the Voltage Dependence of Q_{on}

A simple explanation for the K^+-dependent speeding of gating charge movement at a single membrane potential would be a shift to the left in the voltage dependence of Q_{on}. To test for this, we needed to examine Q_{on} at a series of voltages in the presence of K^+. In wild-type channels, this procedure would also produce contaminating ionic currents. Poorly conducting Kv2.1 channels have been described (Malin and Nerbonne, 2002; Lee et al., 2003). However, a small K^+ conductance remains in these channels, and the reason that these mutant channels conduct poorly is not well un-

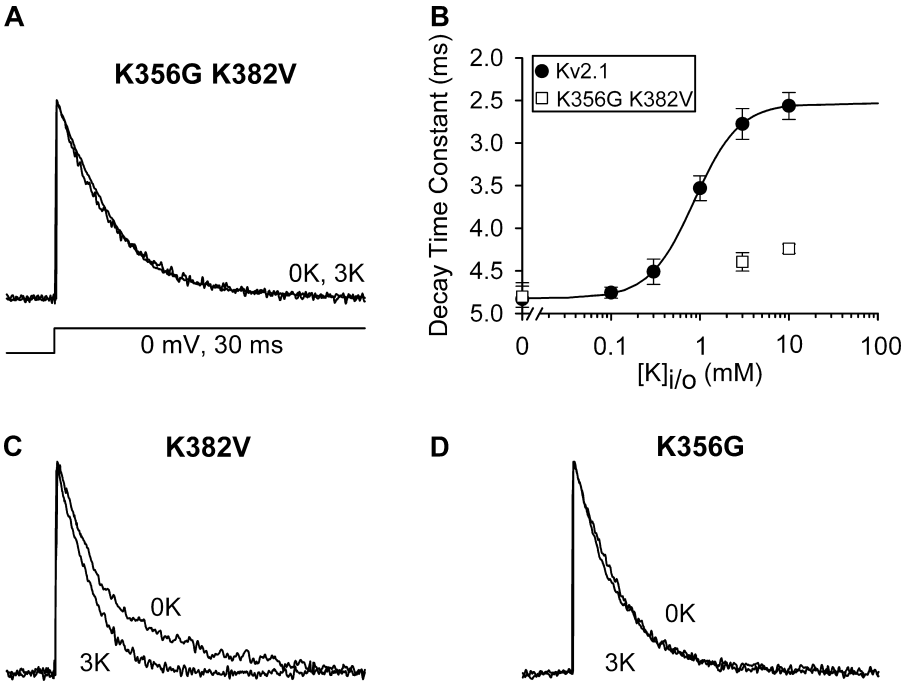

FIGURE 7. K^+-dependent speeding of gating charge movement is abolished by the K356G mutation. (A) Two superimposed (normalized) currents recorded from two different cells that contained the mutant channel Kv2.1 K356G K382V. One current was recorded in the absence of permeant ions, one in the presence of symmetrical 3 mM K^+. Time constants for the current decay in each of these two conditions were: 4.80 ± 0.12 ms (n = 5; 0 K) and 4.39 ± 0.11 ms (n = 4; 3 K). (B) Plot of gating current decay time constant in the presence of different symmetrical [K^+] in wild type Kv2.1 and Kv2.1 K356G K382V. (C) Normalized currents from two cells that contained the mutant channel Kv2.1 K382V. Time constants for the current decay in each of these two conditions were: 4.59 ± 0.06 ms (n = 4; 0 K) and 2.75 ± 0.08 ms (n = 4; 3 K). (D) Normalized currents from two cells that contained the mutant channel Kv2.1 K356G. Time constants for the current decay in each of these two conditions were: 4.45 ± 0.18 ms (n = 4; 0 K) and 4.01 ± 0.11 ms (n = 6; 3 K).

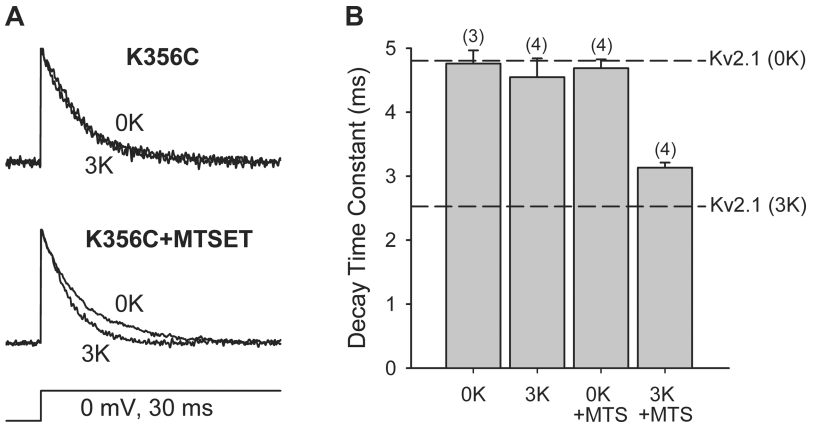

FIGURE 8. Restoration of the K^+-dependent effect on gating current by chemical modification of a cysteine at position 356. (A, top) Normalized gating currents from two cells, one recorded in the absence of permeant ions and one recorded in the presence of symmetrical 3 mM K^+, that contained the mutant channel, Kv2.1 K356C. (A, bottom panel) Similar to A, except that cells were preincubated with 2 mM MTSET for 5 min (B) Plot of decay time constants for currents recorded under the four conditions in A. Bars represent mean ± SEM for the number of cells shown in parentheses. The horizontal dashed lines are drawn at the time constant values obtained at 0 and 3 mM symmetrical K^+ with wild-type Kv2.1 channels.

derstood. Moreover, it is not known whether the mutations that reduce ionic conductance in these channels would influence the physiology that we are studying. Consequently, we chose a different approach to generating Q-V curves in the presence of K^+.

Ionic currents through the Kv2.1 I379C channel can be completely blocked by cysteine-modifying reagents (Kurz et al., 1995). Thus, we chose to examine the Q-V curve in this mutant after complete blockade of ionic current by MTSET. The data in Fig. 9, A and B, demonstrate the feasibility of this approach. Fig. 9 A illustrates four superimposed gating currents from Kv2.1 I379C. One pair of traces illustrates currents recorded in 0 and 3 mM K^+. The rate of gating current decay in this channel in 0 mM K^+ was essentially identical to that in wild-type Kv2.1 (Fig. 9 B). Also similar to the wild-type channel, symmetrical 3 mM K^+ increased the rate of gating charge movement, such that the time constant of gating current decay was similar to that of wild-type Kv2.1 (Fig. 9 B). Elevation of symmetrical [K^+] up to 10 mM produced no additional effect (Fig. 9 B). Modification of the cysteine at position 379 by MTSET had no effect on gating current decay rate with either 0 or 3 mM K^+ (Fig. 9, A and B). Thus, this MTSET-modified channel behaved, almost quantitatively, like wild-type Kv2.1 with respect to the K^+-dependent change in gating current decay.

The inset in Fig. 9 C illustrates the block of ionic current by MTSET when currents were recorded at +40 mV in the presence of symmetrical 3 mM K^+. Fig. 9 C illustrates a family of gating currents evoked from MTSET-modified Kv2.1 I379C, generated by depolarizations between −80 and +60 mV, recorded in the presence of symmetrical 3 mM [K^+]. As is especially apparent from the trace recorded at +60 mV (the largest, fastest current), there was little or no contaminating ionic current in these recordings. Fig. 9 D illustrates full Q-V curves derived from channels, recorded in 0 K^+ (filled squares) and 3 mM symmetrical K^+ after treatment with MTSET (open triangles). The $V_{1/2}$ values were identical, which demonstrates that the speeding of gating charge movement, evident in Fig. 9 A, did not result from a leftward shift in the Q-V curve.

Effect of [K^+] on Voltage Dependence of Gating Current Kinetics

Elevation of [K^+] increased the rates of both gating and ionic current activation, yet had no effect on either the Q-V curve (Fig. 9) or G-V curve (Wood and Korn, 2000). Starace et al. (1997) demonstrated that the S4 domain can shuttle protons across the membrane, and that the rate of proton transport varied with the Q-V relationship. This observation demonstrated that, at a single voltage within the activation range, the net gating current is composed of both a forward and backward transmembrane movement of the S4 domain; the decay of the gating current to 0 represents the achievement of the new steady-state condition. The rate of proton transport, which represented S4 cycling, was greatest near the midpoint of the Q-V curve and decreased to near 0 at the peak of the Q-V curve (Starace et al., 1997). The results described above, wherein the rate of gating charge movement was increased without a concomitant change in the Q-V relationship, would result if elevation of [K^+] were to increase the cycling rate. In this case, the absolute forward and back reaction rates for movement of the S4 domain across the membrane would be increased, but the ratio of the rates would remain the same. This mechanism would also predict that the influence of [K^+] on gating current kinetics would vary with the Q-V. The largest effects would occur near the midpoint of the Q-V (−16 mV), where cycling is greatest, and the effect of [K^+] would diminish near the peak of the Q-V (+30 mV), where the reaction rates approach limits. The experiment in Fig. 10 tested this hypothesis.

Gating currents in Kv2.1 I379C were examined at different membrane potentials under two conditions, 0 mM K^+ (Fig. 10, filled circles) and 3 mM symmetrical K^+ after treatment with MTSET (Fig. 10, open squares). As observed in other K^+ channels (Taglialatela and Stefani, 1993; Islas and Sigworth, 1999;

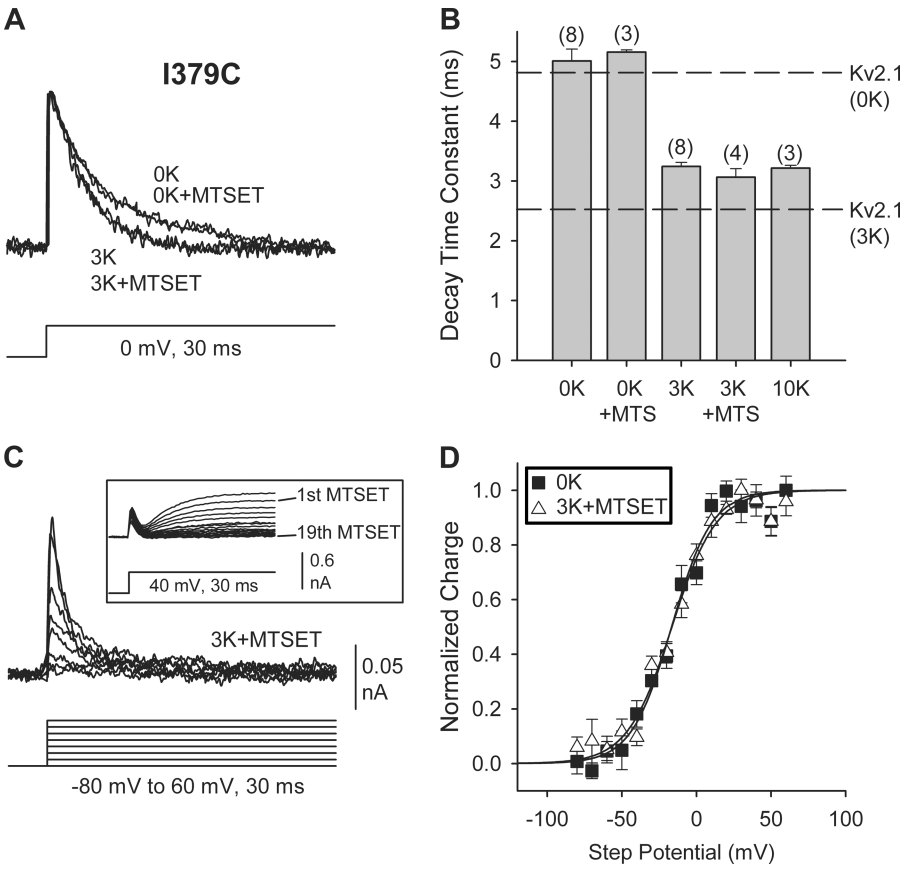

FIGURE 9. K^+ does not speed gating charge movement by shifting voltage-dependence: use of Kv2.1 I379C. (A) Four superimposed (normalized) traces are shown from four different cells containing the mutant channel Kv2.1 I379C. Two traces were recorded in the absence of K^+ (0 K) and two in the presence of symmetrical 3 mM K^+ (3 K). One cell in each of these conditions was recorded after application of 100 μM MTSET to cells for 2 min. In these experiments, MTSET was applied during recording, as in panel C inset. (B) Decay time constants under each of the four conditions in A, in addition to that calculated from currents recorded in the presence of symmetrical 10 mM K^+. Note that at 3 mM K^+, the speeding of gating charge movement had saturated. Bars represent mean ± SEM of number of cells shown in parentheses. Horizontal lines illustrate decay time constants obtained from Kv2.1 at 0 and 3 mM K^+. (C) Family of gating currents from a single cell, obtained by depolarization to potentials between −80 and +60 mV after preincubation with 100 μM MTSET for 2 min. (Inset) Illustration of block of ionic current by application of 100 μM MTSET, from a cell recorded in symmetrical 3 mM K^+. (D) Q-V curve from Kv2.1 I379C under two conditions: in the absence of K^+ (no MTSET treatment) and in the presence of symmetrical 3 mM K^+ after pretreatment with MTSET. Calculated $V_{1/2}$ values were −16.6 ± 2.7 mV (n = 3) and −16.4 ± 1.9 mV (n = 3). Slope values were 13.4 and 14.9.

Ledwell and Aldrich, 1999), gating current kinetics slowed between −40 and −10 mV and then increased in rate with additional depolarization (Fig. 10 A). The largest effect of K^+ on gating current kinetics occurred near −10 mV, the approximate midpoint of the Q-V. The effect progressively decreased until, near +30 mV, elevation of [K^+] had no influence on the gating current. Fig. 10 B illustrates the same data, plotted semilogarithically. With both 0 and 3 mM K^+, the time constant of gating current decay was well fit by a linear function between −10 and +50 mV. At +60 mV, the kinetics of the gating current appeared to approach saturation, which suggests that regardless of voltage or [K^+], the forward rate of voltage sensor movement was approaching a limit.

The biphasic data in Fig. 10 A, together with the demonstrated cycling of the S4 domain (Starace et al., 1997), is consistent with a simple two state model of gating current kinetics, consisting of a forward and backward first order reaction (although a more complicated model is undoubtedly necessary for a precise description of gating current kinetics [c.f. Schoppa and Sigworth, 1998], this simplified model is appropriate given our data and purpose of this analysis). From the Q-V curve (Fig. 9), and the time constant values at different voltages (Fig. 10 A), we calculated the forward and backward rate constants (α and β) for this model, from: $Q_{norm} = \alpha/(\alpha + \beta)$ and $Tau = 1/(\alpha + \beta)$. The log values of α and β are plotted as a function of voltage in Fig. 10, C and D. As expected for this two state model, the value of α increased, and the value of β decreased, as a function of increasing depolarization. Elevation of [K^+] increased the values of both α and β. The largest effect of K^+ on both α and β occurred at more negative potentials (near the midpoint of the Q-V). At the most positive potentials, K^+ had little (Fig. 10 D) or no (Fig. 10 C) effect on the rate constants. Although the absolute values of both α and β were increased by K^+, there was virtually no effect on the ratio of α to β (Fig. 10 E). All of these data are consistent with a mechanism whereby elevation of [K^+] decreased an energy barrier for voltage sensor movement, and thus increased the rate of voltage sensor cycling.

Association of Ionic and Gating Current Activation Rates

Fig. 11 A illustrates ionic currents activated by depolarization to +40 mV in the presence of symmetrical 0.3 mM and 10 mM [K^+]. The complete [K^+] dependence

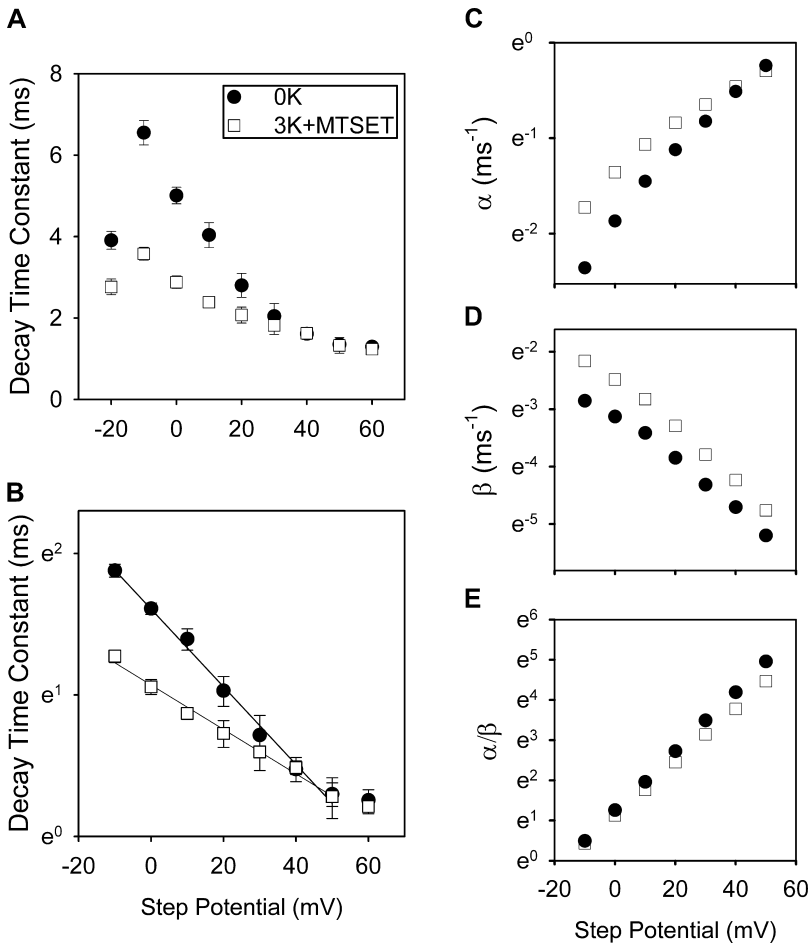

FIGURE 10. [K^+]-dependent change in Q_{on} kinetics as a function of voltage. Gating currents were recorded in Kv2.1 I379C under two conditions: 0 internal and external K^+ (filled circles) and 3 mM symmetrical K^+ plus MTSET (open squares). (A) Decay time constant as a function of voltage. Each data point represents the mean of measurements obtained from 3 to 13 cells. (B) Semilogarithmic plot of the data in A. Linear regression curves were fit for data between −10 and +50 mV. (C and D) α and β as a function of voltage, calculated as described in the text. (E) Ratios of α and β, from the data in C and D.

of ionic current activation rate is plotted in Fig. 11 B (open triangles). Superimposed on this plot is the [K^+] dependence of the gating current time constant (filled circles). The [K^+] dependence of these two effects was identical, which supports the conclusion that the change in ionic current activation rate can be accounted for by the change in rate of voltage sensor movement. Thus, these data strongly support the conclusion that K^+ in the pore, at a specific site in the selectivity filter, alters the rate of movement of the voltage sensor, and that this change is translated into a change in the rate of ionic current activation.

DISCUSSION

In the Kv2.1 potassium channel, elevation of external [K^+] between 0 and 10 mM produces a concentration-dependent increase in outward current magnitude, activation rate, and inactivation rate (Immke et al., 1999; Wood and Korn, 2000). The elevation in [K^+] also changes both internal and external TEA sensitivity of the channel (Immke et al., 1999; Immke and Korn, 2000). The changes in current magnitude and external TEA sensitivity were attributed to the reorientation of an outer vestibule lysine within the conduction pathway, which occurred as a consequence of a change in K^+ occupancy of a specific selectivity filter site (Immke et al., 1999; Immke and Korn, 2000; Wood and Korn, 2000). Consequently, in one conformation, which exists when K^+ occupies this selectivity filter site, currents through the channel are larger and activate and inactivate faster (Immke et al., 1999; Wood and Korn, 2000). In the other conformation, which occurs when this selectivity filter site is not occupied by K^+, currents are smaller and display slower activation and inactivation kinetics. Transition between these two outer vestibule conformations is not dynamic during the conduction process; once open, channels do not change conformation (Andalib et al., 2002).

The experiments in this paper indicate that binding of K^+ to the selectivity filter site that controls outer vestibule conformation also influences the rate of on-gating charge movement. Four lines of evidence strongly support the conclusion that the change in rate of Q_{on} was directly associated with the K^+-dependent change in outer vestibule conformation. First, the change in rate of Q_{on} occurred over the same range of [K^+] that produced a switch in outer vestibule conformation, as measured by changes in channel pharmacology and

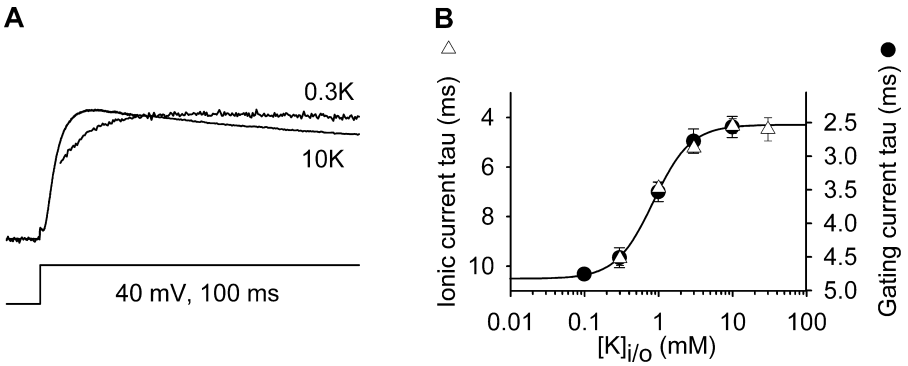

FIGURE 11. [K^+]-dependent increase in rate of ionic current activation. (A) Superimposed, (normalized) ionic currents from Kv2.1 recorded at +40 mV in the presence of symmetrical 0.3 mM K^+ and 10 mM K^+. Peak current magnitudes were 110 pA (0.3K) and 4,400 pA (10K). Due to the large transient, the first 5 ms of the 0.3 mM K^+ current were blanked. (B) Plots of time constants of ionic current activation and gating current decay at different symmetrical [K^+]. Data represent mean ± SEM of 4–6 cells.

ionic current properties. Second, experimental manipulations that produced or eliminated the outer vestibule–based effects on channel pharmacology and ionic currents similarly altered the K^+-dependent effects on Q_{on}. Third, Rb^+ and Cs^+ influenced the outer vestibule conformation over the same concentration range as they influenced the rate of Q_{on} (compare Figs. 3 B and 5). Most tellingly, however, while Rb^+ and K^+ altered these two functional parameters over the same concentration range, Cs^+ altered these two functional parameters over a dramatically different range (Figs. 3 B and 5). Fourth, the specificity of this site was further demonstrated by the observation that Cs^+ bound to the selectivity filter at a much lower concentration than required to affect either outer vestibule conformation or Q_{on} (Fig. 4). Thus, it was not merely the occupancy of any selectivity filter site that influenced gating charge movement. Together, these data strongly indicate that the different rates of gating charge movement resulted from [K^+]-dependent differences in outer vestibule conformation.

Experiments that demonstrated identical [K^+] dependence and identical effects of mutations on gating and ionic currents suggest that this increased rate of gating charge movement can fully account for the increased rate of ionic current activation.

Ions in the Pore and Gating

In voltage-gated K^+ channels, permeant ions in the conduction pathway influence a number of gating processes. The presence of ions in the pore can slow deactivation (Swenson and Armstrong, 1981; Cahalan et al., 1985; Matteson and Swenson, 1986, Sala and Matteson, 1991), speed opening rate (Neyton and Pelleschi, 1991; Demo and Yellen, 1992), slow inactivation in channels that undergo classical C-type inactivation (Lopez-Barneo et al., 1993; Baukrowitz and Yellen, 1996; Kiss and Korn, 1998), and speed recovery from this same inactivation mechanism (Levy and Deutsch, 1996). The slowing of deactivation was most easily interpreted as an inability of the activation gate to close with an ion located somewhere inside the pore. Similarly, the influence of K^+ on opening rate was most easily explained as a destabilization of the closed state when an ion occupied a site in the pore, possibly at the selectivity filter (Neyton and Pelleschi, 1991; Demo and Yellen, 1992). The slowing of C-type inactivation by K^+ is thought to be due to a "foot-in-the-door" mechanism, by which K^+ located at the selectivity filter prevents the local constriction of the pore that produces inactivation (Baukrowitz and Yellen, 1996; Liu et al., 1996; Kiss and Korn, 1998; Kiss et al., 1999). Similarly, the speeding of recovery from inactivation is most easily explained as a destabilization of the inactivated (constricted) conformation of the channel by K^+ from inside of the pore (Levy and Deutsch, 1996). Thus, K^+ at some location within the constricted pore appears to encourage the deconstriction of the outer mouth of the pore. Consequently, all of these previously observed effects of permeant ions on gating are most easily explained as resulting from an interaction of K^+ with gates inside of the conduction pathway.

In contrast to these previously observed effects, our data indicate that permeant ions inside of the conduction pathway of Kv2.1 can influence gating by changing the operation of the voltage sensor, which is outside of the conduction pathway. Although several regions within the S1-S4 span of the channel are involved in the gating process, the charged residues that make up the gating current are located primarily in the S4 domain (Aggarwal and MacKinnon, 1996; Seoh et al., 1996). Moreover, although other channel domains may move during activation (Milligan and Wray, 2000; Jiang et al., 2003), the fundamental protein movement that underlies gating charge movement appears to be the outward translocation of the S4 domain (Larsson et al., 1996; Yang et al., 1996; Starace et al., 1997; Jiang et al., 2003). Thus, the increased rate of gating charge movement associated with K^+ occupancy of the selectivity filter most likely reflects the increased rate of translocation of the S4 domain. Starace et al. (1997) demonstrated that, upon depolarization, the S4 domain cycles between an

inward and outward position, relative to the plasma membrane. Thus, the decay of the gating current to 0 reflects the time it takes to achieve a new steady-state level of cycling. The data in Fig. 10 suggest that K^+ speeds the rate of gating charge movement by lowering an energy barrier for voltage sensor movement and thus increasing the cycling of the S4 domain across the membrane.

Potential Location of Interaction between S4 and the Pore

A large portion of the Kv2.1 channel, ranging from the turret in the outer vestibule to the channel region internal to the selectivity filter, undergoes a reorientation as a function of K^+ occupancy of the selectivity filter (Immke et al., 1999). As with the other changes in channel function associated with this K^+-dependent reorientation, the modulation of voltage sensor movement requires the presence of a positive charge at a specific turret location (356 in Kv2.1). Because the conformational change internal to the selectivity filter still occurs after neutralization of position 356 (Immke et al., 1999), it appears unlikely that manipulation of position 356 influences voltage sensor movement at this remote location. Rather, it appears that the functional changes upon manipulation of position 356 are produced locally (also, see below). Indeed, several studies have demonstrated an intimate juxtaposition between the S4 domain and the turret (Loots and Isacoff, 2000; Elinder et al., 2001a,b; Broomand et al., 2003; Gandhi et al., 2003; Laine et al., 2003; Neale et al., 2003), which supports the conclusion that the interaction between the voltage sensor and the conduction pathway occurs in the region of the turret. Our hypothesis, therefore, is that the rate of S4 translocation in Kv2.1 is directly influenced by the conformation of the outer vestibule, which takes on one of two orientations depending on the occupancy of a selectivity filter site by K^+.

An alternative possibility, that the effect of K^+ on gating charge movement was transmitted allosterically via the activation gate located in the cytoplasmic end of the channel, seems unlikely for several reasons. First, neither K^+ nor the outer vestibule mutations influenced the voltage dependence of activation of either gating or ionic current (Figs. 6 and 9; Wood and Korn, 2000). These results suggest that the function of the cytoplasmic gate, and the coupling between this gate and the voltage sensor, were unaffected by these manipulations. Second, it is not clear how a selective mutation of one amino acid residue (K356) in the turret of the outer vestibule could abolish the effect of K^+ on Q_{on}, nor how chemical modification of K356C in the outer vestibule by MTSET could reinstate the K^+-dependent speeding of Q_{on}, if the effect of K^+ were transmitted via the internal gate with no involvement of the outer vestibule. Third, the influence of K^+ on voltage sensor movement depended specifically on the occupancy of a selectivity filter site that is responsible for the switching of outer vestibule conformation.

Conclusion

The outer vestibule is clearly involved in channel inactivation, and appears to be involved in the activation process as well. Several recent studies have demonstrated that the S4 domain is quite near the outer vestibule turret, and that during activation, it moves even closer to the turret. Our data indicate that the conformation of the outer vestibule, which is dynamic and modulatable in at least the Kv2.1 potassium channel, can influence both the mobility of the S4 domain and the activation kinetics of ionic current. Moreover, the reorientation of the outer vestibule that influences S4 movement occurs with physiologically relevant changes in external $[K^+]$ (Immke and Korn, 2000), and may be especially relevant when internal K^+ channel blockers are present (Wood and Korn, 2000).

We thank Dr. Richard Horn for illuminating discussions about gating machinery and kinetics.

Supported by NIH NS41090.

Olaf S. Andersen served as editor.

Submitted: 6 January 2004
Accepted: 20 February 2004

REFERENCES

Aggarwal, S.K., and R. MacKinnon. 1996. Contribution of the S4 segment to gating charge in the *Shaker* K^+ channel. *Neuron.* 16: 1169–1177.

Andalib, P., M.J. Wood, and S.J. Korn. 2002. Control of outer vestibule dynamics and current magnitude in the Kv2.1 potassium channel. *J. Gen. Physiol.* 120:739–755.

Armstrong, C.M., and B. Hille. 1972. The inner quaternary ammonium ion receptor in potassium channels of the Node of Ranvier. *J. Gen. Physiol.* 59:388–400.

Armstrong, C.M., and F. Bezanilla. 1974. Charge movement associated with the opening and closing of the activation gates of the Na channels. *J. Gen. Physiol.* 63:533–552.

Bao, H., A. Hakeem, M. Henteleff, J.G. Starkus, and M.D. Rayner. 1999. Voltage-insensitive gating after charge-neurtalizing mutations in the S4 segment of *Shaker* channels. *J. Gen. Physiol.* 113: 139–151.

Baukrowitz, T., and G. Yellen. 1996. Use-dependent blockers and exit rate of the last ion from the multi-ion pore of a K^+ channel. *Science.* 271:653–656.

Broomand, A., R. Mannikko, H.P. Larsson, and F. Elinder. 2003. Molecular movement of the voltage sensor in a K channel. *J. Gen. Physiol.* 122:741–748.

Cahalan, M.D., K.G. Chandy, T.E. DeCoursey, and S. Gupta. 1985. A voltage-gated potassium channel in human T lymphocytes. *J. Physiol.* 358:197–237.

Cha, A., and F. Bezanilla. 1997. Characterizing voltage-dependent conformational changes in the *Shaker* K^+ channel with fluorescence. *Neuron.* 19:1127–1140.

del Camino, D., and G. Yellen. 2001. Tight steric closure at the intracellular activation gate of a voltage-gated K^+ channel. *Neuron.* 32:649–656.

Demo, S.D., and G. Yellen. 1992. Ion effects on gating of the Ca^{2+}-activated K^+ channel correlate with occupancy of the pore. *Biophys. J.* 61:639–648.

Ding, S., and R. Horn. 2003. Effect of S6 tail mutations on charge movement in *Shaker* potassium channels. *Biophys. J.* 84:295–305.

Elinder, F., P. Arhem, and H.P. Larsson. 2001a. Localization of the extracellular end of the voltage sensor S4 in a potassium channel. *Biophys. J.* 80:1802–1809.

Elinder, F., R. Mannikko, and H.P. Larsson. 2001b. S4 charges move close to residues in the pore domain during activation in a K channel. *J. Gen. Physiol.* 118:1–10.

Flynn, G.E., and W.N. Zagotta. 2001. Conformational changes in S6 coupled to the opening of cyclic nucleotide-gated channels. *Neuron.* 30:689–698.

Gandhi, C.S., E. Clark, E. Loots, A. Pralle, and E.Y. Isacoff. 2003. The orientation and molecular movement of a K^+ channel voltage-sensing domain. *Neuron.* 40:515–525.

Hackos, D.H., T.-H. Chang, and K.J. Swartz. 2002. Scanning the intracellular S6 activation gate in the Shaker K^+ channel. *J. Gen. Physiol.* 119:521–531.

Hodgkin, A.L., and A.F. Huxley. 1952. A quantitative description of membrane current and its application to conduction and excitation in nerve. *J. Physiol.* 117:500–544.

Holmgren, M., P.L. Smith, and G. Yellen. 1997. Trapping of organic blockers by closing of voltage-dependent K^+ channels. Evidence for a trap door mechanism of activation gating. *J. Gen. Physiol.* 109:527–535.

Holmgren, M., K.S. Shin, and G. Yellen. 1998. The activation gate of a voltage-gated K^+ channel can be trapped in the open state by an intersubunit metal bridge. *Neuron.* 21:617–621.

Ikeda, S.R., and S.J. Korn. 1995. Influence of permeating ions on potassium channel block by external tetraethylammonium. *J. Physiol.* 486:267–272.

Immke, D., M.J. Wood, L. Kiss, and S.J. Korn. 1999. Potassium-dependent changes in the conformation of the Kv2.1 potassium channel pore. *J. Gen. Physiol.* 113:819–836.

Immke, D., and S.J. Korn. 2000. Ion-ion interactions at the selectivity filter: evidence from K^+-dependent modulation of tetraethylammonium efficacy in Kv2.1 potassium channels. *J. Gen. Physiol.* 115:509–518.

Islas, L.D., and F.J. Sigworth. 1999. Voltage sensitivity and gating charge in *Shaker* and *Shab* family potassium currents. *J. Gen. Physiol.* 114:723–741.

Jiang, Y., V. Ruta, J. Chen, A. Lee, and R. MacKinnon. 2003. The principle of gating charge movement in a voltage-dependent K^+ channel. *Nature.* 423:42–48.

Jurman, M.E., L.M. Boland, Y. Liu, and G. Yellen. 1994. Visual identification of individual transfected cells for electrophysiology using antibody-coated beads. *Biotechniques.* 17:876–881.

Kiss, L., and S.J. Korn. 1998. Modulation of C-type inactivation by K^+ at the potassium channel selectivity filter. *Biophys. J.* 74:1840–1849.

Kiss, L., J. LoTurco, and S.J. Korn. 1999. Contribution of the selectivity filter to inactivation in potassium channels. *Biophys. J.* 76: 253–263.

Kurz, L., R.D. Zuhlke, H.-J. Zhang, and R.H. Joho. 1995. Side-chain accessibilities in the pore of a K^+ channel probed by sulfhydryl-specific reagents after cysteine scanning mutagenesis. *Biophys. J.* 68:900–905.

Laine, M., M.-C.A. Lin, J.P.A. Bannister, W.R. Silverman, A.F. Mock, B. Roux, and D.M. Papazian. 2003. Atomic proximity between S4 segment and pore domain in Shaker potassium channels. *Neuron.* 39:467–481.

Larsson, H.P., O.S. Baker, D.S. Dhillon, and E.Y. Isacoff. 1996. Transmembrane movement of the *Shaker* K^+ channel S4. *Neuron.* 16:387–397.

Ledwell, J.L., and R.W. Aldrich. 1999. Mutations in the S4 region isolate the final voltage-dependent cooperative step in potassium channel activation. *J. Gen. Physiol.* 113:389–414.

Lee, H.C., J.M. Wang, and K.J. Swartz. 2003. Interaction between extracellular hanatoxin and the resting conformation of the voltage-sensor paddle in Kv channels. *Neuron.* 40:527–536.

Levy, D.I., and C. Deutsch. 1996. Recovery from C-type inactivation is modulated by extracellular potassium. *Biophys. J.* 70:798–805.

Liu, Y., M.E. Jurman, and G. Yellen. 1996. Dynamic rearrangement of the outer mouth of a K^+ channel during gating. *Neuron.* 16: 859–867.

Liu, Y., M. Holmgren, M.E. Jurman, and G. Yellen. 1997. Gated access to the pore of a voltage-dependent K^+ channel. *Neuron.* 19: 175–184.

Liu, Y., and R.H. Joho. 1998. A side chain in S6 influences both open-state stability and ion permeation in a voltage-gated K^+ channel. *Pflugers Arch.* 435:654–661.

Lopez-Barneo, J., T. Hoshi, S.H. Heinemann, and R.W. Aldrich. 1993. Effects of external cations and mutations in the pore region on C-type inactivation of *Shaker* potassium channels. *Receptors Channels.* 1:61–71.

Loots, E., and E.Y. Isacoff. 2000. Molecular coupling of S4 to a K^+ channel's slow inactivation gate. *J. Gen. Physiol.* 116:623–635.

Lu, T., L.W. Wu, J. Xiao, and J. Yang. 2001a. Permeant ion-dependent changes in gating of Kir2.1 inward rectifier potassium channels. *J. Gen. Physiol.* 118:509–521.

Lu, T., A.Y. Ting, J. Mainland, L.Y. Jan, P.G. Schultz, and J. Yang. 2001b. Probing ion permeation and gating in a K^+ channel with backbone mutations in the selectivity filter. *Nat. Neurosci.* 4:239–246.

Lu, Z., A.M. Klem, and Y. Ramu. 2002. Coupling between voltage sensors and activation gate in voltage-gated K^+ channels. *J. Gen. Physiol.* 120:663–676.

Malin, S.A., and J.M. Nerbonne. 2002. Delayed rectifier K+ currents, IK, are encoded by Kv2 α-subunits and regulate tonic firing in mammalian sympathetic neurons. *J. Neurosci.* 22:10094–10105.

Matteson, D.R., and R.P. Swenson, Jr. 1986. External monovalent cations that impede the closing of K channels. *J. Gen. Physiol.* 87: 795–816.

Milligan, C.J., and D. Wray. 2000. Local movement in the S2 region of the voltage-gated potassium channel hKv2.1 studied using cysteine mutagenesis. *Biophys. J.* 78:1852–1861.

Neale, E.J., D.J.S. Elliott, M. Hunter, and A. Sivaprasadarao. 2003. Evidence for intersubunit interactions between S4 and S5 transmembrane segments of the Shaker potassium channel. *J. Biol. Chem.* 278:29079–29085.

Neyton, J., and M. Pelleschi. 1991. Multi-ion occupancy alters gating in high conductance Ca^{2+}-activated K^+ channels. *J. Gen. Physiol.* 97:641–665.

Proks, P., J.F. Antcliff, and F.M. Ashcroft. 2003. The ligand-sensitive gate of a potassium channel lies close to the selectivity filter. *EMBO Rep.* 4:70–75.

Sala, S., and D.R. Matteson. 1991. Voltage-dependent slowing of K channel closing kinetics by Rb^+. *J. Gen. Physiol.* 98:535–554.

Schoppa, N.E., and F.J. Sigworth. 1998. Activation of *Shaker* potassium channels. III. An activation gating model for wild-type and V2 mutant channels. *J. Gen. Physiol.* 111:313–342.

Seoh, S.-A., D. Sigg, and F. Bezanilla. 1996. Voltage-sensing residues in the S2 and S4 segments of the *Shaker* K^+ channel. *Neuron.* 16: 1159–1167.

So, I., I. Ashmole, N.W. Davies, M.J. Sutcliffe, and P.R. Stanfield. 2001. The K^+ channel signature sequence of murine Kir2.1: mutations that affect microscopic gating but not ionic selectivity. *J. Physiol.* 531:37–50.

Starace, D.M., E. Stefani, and F. Bezanilla. 1997. Voltage-dependent proton transport by the voltage sensor of the *Shaker* K^+ channel. *Neuron*. 19:1319–1327.

Sun, Z.-P., M.H. Akabas, E.H. Goulding, A. Karlin, and S.A. Siegelbaum. 1996. Exposure of residues in the cyclic nucleotide-gated channel pore: P region structure function in gating. *Neuron*. 16: 141–149.

Swenson, R.P., Jr., and C.M. Armstrong. 1981. K^+ channels close more slowly in the presence of external K^+ and Rb^+. *Nature*. 291: 427–429.

Taglialatela, M., and E. Stefani. 1993. Gating currents of the cloned delayed-rectifier K^+ channel DRK1. *Proc. Natl. Acad. Sci. USA*. 90: 4758–4762.

Tristani-Firouzi, M., J. Chen, and M.C. Sanguinetti. 2002. Interactions between S4-S5 linker and S6 transmembrane domain modulate gating of HERG K^+ channels. *J. Biol. Chem*. 277:18994–19000.

Wang, Z., J.C. Hesketh, and D. Fedida. 2000. A high Na^+ conduction state during recovery from inactivation in the K^+ channel Kv1.5. *Biophys. J*. 79:2416–2433.

Wood, M.J., and S.J. Korn. 2000. Two mechanisms of K^+-dependent potentiation in Kv2.1 potassium channels. *Biophys. J*. 79:2535–2546.

Yang, N., A.L. George, Jr., and R. Horn. 1996. Molecular basis of charge movement in voltage-gated sodium channels. *Neuron*. 16: 113–122.

Yellen, G., D. Sodickson, T.-Y. Chen, and M.E. Jurman. 1994. An engineered cysteine in the external mouth of a K^+ channel allows inactivation to be modulated by metal binding. *Biophys. J*. 66: 1068–1075.

Zheng, J., and F.J. Sigworth. 1998. Intermediate conductances during deactivation of heteromultimeric *Shaker* potassium channels. *J. Gen. Physiol*. 112:457–474.

Zhou, Y., J.H. Morais-Cabral, A. Kaufman, and R. MacKinnon. 2001. Chemistry of ion coordination and hydration revealed by a K^+ channel–Fab complex at 2.0 Å resolution. *Nature*. 414:43–48.